Bioorganic & Medicinal Chemistry 18 (2010) 5466–5474

Contents lists available at ScienceDirect

Bioorganic & Medicinal Chemistry

journal homepage: www.elsevier.com/locate/bmc

Baculiferins A–O, O-sulfated pyrrole alkaloids with anti-HIV-1 activity, from the Chinese marine sponge *Iotrochota baculifera*

Guotao Fan [a], Zelin Li [b,*], Shi Shen [a], Yi Zeng [b], Yishu Yang [b], Minjuang Xu [a], Torsten Bruhn [c], Heike Bruhn [d], Joachim Morschhäuser [d], Gerhard Bringmann [c,*], Wenhan Lin [a,*]

[a] *State Key Laboratory of Natural and Biomimetic Drugs, Peking University, Beijing 100083, People's Republic of China*
[b] *College of Life Science and Bioengineering, Beijing University of Technology, Beijing 100022, People's Republic of China*
[c] *Institute of Organic Chemistry, University of Würzburg, Am Hubland, D-97074 Würzburg, Germany*
[d] *Institute for Molecular Infection Biology, University of Würzburg, Josef-Schneider-Str. 2, D-97080 Würzburg, Germany*

ARTICLE INFO

Article history:
Received 13 May 2010
Revised 16 June 2010
Accepted 17 June 2010
Available online 23 June 2010

Keywords:
Marine sponge
Iotrochota baculifera
Baculiferins A–O
HIV-1 target proteins
HIV-1 IIIB virus

ABSTRACT

Fifteen new DOPA-derived pyrrole alkaloids, named baculiferins A–O (**2**–**16**), were isolated from the Chinese marine sponge *Iotrochota baculifera*, together with the known alkaloids purpurone (**1**) and ningalin A (**17**). Most of the new compounds contain one to three O-sulfate units. Their structures were determined by extensive spectroscopic analysis including ^{1}H and ^{13}C NMR (COSY, HMQC, HMBC) and ESIMS data. A possible pathway for the biosynthetic origin of the isolated alkaloids is proposed, in which DOPA is assumed to be a joint biogenetic precursor. Baculiferins C, E–H, and K–N (**4**, **6**–**9**, **12**–**15**) were found to be potent inhibitors against the HIV-1 IIIB virus in both, MT4 and MAGI cells. Additional bioassay revealed that baculiferins could dramatically bind to the HIV-1 target proteins Vif, APOBEC3G, and gp41, for which structure–activity relationships are discussed.

1. Introduction

The amino acid DOPA [2-amino-3-(3′,4′-dihydroxyphenyl) propionic acid] is increasingly recognized as a key precursor to a broad variety of structurally unique alkaloids in marine invertebrates.[1–4] These DOPA-derived alkaloids are naturally occurring polyaromatic molecules with a pyrrole core, differing by the substitution pattern and the arrangement of the rings. They can be classified into the subtypes of lamellarins, lukianols, polycitrins, polycitons, storniamides, and ningalins, based on the cyclic condensation and the ring composition surrounding the pyrrole ring as a central unit. More than 70 such DOPA-derived pyrrole alkaloids have been reported from diverse marine organisms (mollusks, ascidians, and sponges).[3] Lamellarins are featured with a benzopyrano-pyrrolo-isoquinolinone nucleus;[2,5–15] lukianols mainly consist of a naturally rare *N*-alkylpyrrolecarboxylic acid;[16] polyxitones and polycitons are a small group with an unprecedented molecular skeleton[6,17] assumed to be biogenetically derived from lamellarins; storniamides are of peptide origin,[16] while ningalins, among them purpurone (**1**, see Fig. 1)[18,19] and ningalin A (**17**),[18] are derived from the condensation of two, three, four, or five DOPA precursor units. The DOPA-derived alkaloids exhibit a wide array of significant biological activities, including cytotoxicity, HIV-1 integrase inhibition,[20] multidrug resistance reversal activity[21] and immunomodulatory activity. Although marine sponges are known to be a rich source of structurally unique and biologically active secondary metabolites, DOPA-derived alkaloids are only found in the Patagonian sponge *Cliona* sp. (storniamides A–D) and in the Pacific Ocean sponge *Iotrochota* sp. (purpurone). Purpurone (**1**) is a polycatecholic pyrrole and is closely related to ningalin D, which was also isolated from an ascidian of the genus *Didemnum*.[19] It inhibits ATP-citrate lyase in a dose-dependent manner. The DOPA-derived polyaromatic alkaloids with an unsymmetrical skeleton, such as ningalins B and C have previously been found only in the ascidian genus *Didemnum*.[19] As part of our interest in the chemical diversity of Chinese marine sponges, the species *Iotrochota baculifera,* which is indigenous to the reef Bay of Hainan Island, was collected. From this material, 15 new purpurone related alkaloids were isolated and characterized, mostly sulfated pyrrole alkaloids, named baculiferins A–O (**2**–**16**), together with purpurone (**1**) and ningalin A (**17**).

* Corresponding authors. Tel.: +86 10 82806188; fax: +86 10 82802724 (W.L.).
E-mail addresses: bringman@chemie.uni-wuerzburg.de (G. Bringmann), whlin@bjmu.edu.cn (W. Lin).

0968-0896/$ - see front matter © 2010 Elsevier Ltd. All rights reserved.
doi:10.1016/j.bmc.2010.06.052

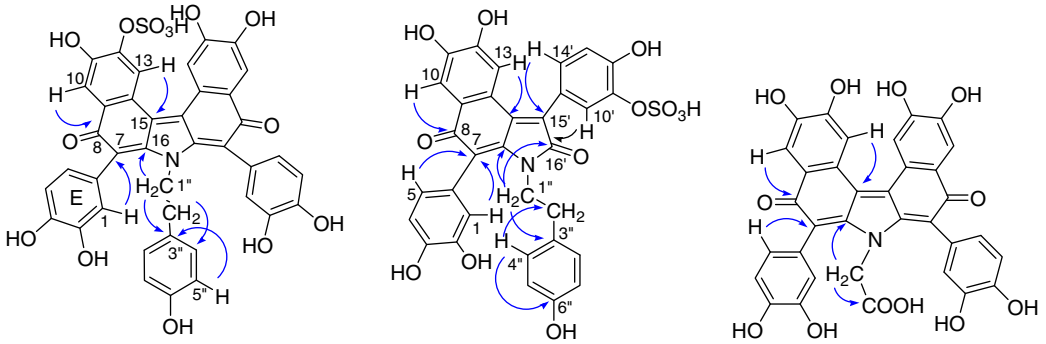

2 **10** **13**

Figure 1. Key HMBC correlations in **2**, **10**, and **13**.

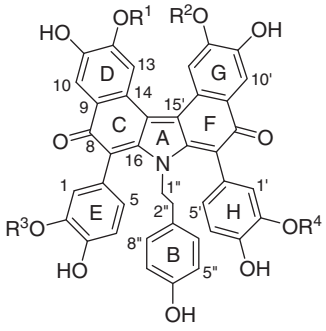

1 $R^1 = R^2 = R^3 = R^4 = H$ (purpurone)
2 $R^1 = SO_3H$, $R^2 = R^3 = R^4 = H$ (baculiferin A)
3 $R^3 = SO_3H$, $R^1 = R^2 = R^4 = H$ (baculiferin B)
4 $R^3 = R^4 = SO_3H$, $R^1 = R^2 = H$ (baculiferin C)
5 $R^1 = R^2 = SO_3H$, $R^3 = R^4 = H$ (baculiferin D)
6 $R^1 = R^3 = SO_3H$, $R^2 = R^4 = H$ (baculiferin E)
7 $R^1 = R^4 = SO_3H$, $R^2 = R^3 = H$ (baculiferin F)
8 $R^1 = R^3 = R^4 = SO_3H$, $R^2 = H$ (baculiferin G)
9 $R^1 = R^2 = R^3 = SO_3H$, $R^4 = H$ (baculiferin H)

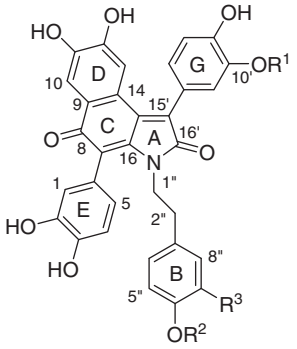

10 $R^1 = SO_3H$, $R^2 = R^3 = H$ (baculiferin I)
11 $R^1 = H$, $R^2 = SO_3H$, $R^3 = H$ (baculiferin J)
12 $R^1 = R^2 = R^3 = H$ (baculiferin K)
$R^1 = R^2 = H$, $R^3 = OH$ (ningalin C)

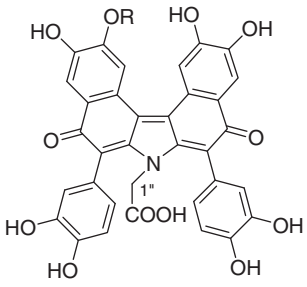

13 R = H (baculiferin L)
14 R = SO_3H (baculiferin M)

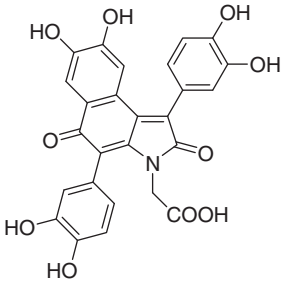

15 (baculiferin N)

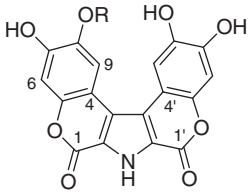

16 R = SO_3H (baculiferin O)
17 R = H (ningalin A)

2. Results and discussion

The frozen sponge *I. baculifera* (600 g, wet wt) was homogenized and extracted with 95% EtOH. The EtOH extract was partitioned between H_2O and EtOAc and then *n*-BuOH. The dark-red *n*-BuOH fraction was repeatedly chromatographed by semi-preparative HPLC (ODS) in association with a separation on a Sephadex LH-20 column to afford 15 new purpurone derivatives, baculiferins A–O (**2**–**16**), and two known compounds, **1** and **17**. Purpurone (**1**) had already been isolated from the same sponge species,[16] and ningalin A (**17**)[18] had been obtained for the first time from the sponge genus *Iotrochota*.

Baculiferin A (**2**) was isolated as a dark-red amorphous solid. It was found to possess a molecular formula of $C_{40}H_{27}NO_{14}S$ as determined by HRESIMS (*m/z* 776.1072 $[M-H]^-$, calcd 776.1079) in negative-ion mode, implying 28 degrees of unsaturation. The UV bands at 262, 274, 327, and 508 nm, along with the IR absorptions at 3418–3000, 1702, and 1670 cm^{-1}, suggested the presence of

hydroxy, carbonyl, and conjugated polyene groups. The ^{13}C NMR spectrum displayed a total of 34 resonances, most of them present in aromatic region around δ 142–154 and in the region between δ 114 and 129, with the exception of two conjugated ketones at δ 183–184, and two aliphatic methylenes at δ 33.3 (t) and 46.5 (t). The ^1H NMR spectrum exhibited two aromatic ABX spin systems overlapped at δ 6.86 (2H, d, J = 1.5 Hz, H-1, 1′), 6.83 (2H, d, J = 8.0 Hz, H-4, 4′), and 6.72 (2H, dd, J = 1.5, 8.0 Hz, H-5,5′); an AA′BB′ spin system at δ 6.38 (2H, d, J = 7.5 Hz) and 6.48 (2H, d, J = 7.5 Hz), four aromatic singlets at δ 7.58 (1H, s), 7.48 (1H, s), 8.56 (1H, s), and 8.02 (1H, s), along with two vicinal-coupled methylenes at δ 2.22 (2H, t, J = 6.5 Hz) and 2.99 (2H, t, J = 6.5 Hz). The ^1H and ^{13}C NMR spectroscopic data of **2** (Tables 1 and 2) were closely related to those of purpurone (**1**), indicating a purpurone-type analogue. A difference was found in the two annulated rings, where the chemical shifts of H-10 (δ 7.58, s) and H-13 (δ 8.56, s) of ring D varied from those of H-10′ (δ 7.48, s) and H-13′ (δ 8.02, s) of ring G. These findings evidenced unsymmetrical substitution patterns between the two aromatic rings. The HMQC and HMBC data (Fig. 1) revealed that the resonance of C-12 was shifted upfield to δ 142.6 (s), whereas C-11 and C-13 were shifted downfield to δ 150.9 (s) and 120.5 (d), as compared to the signals of C-11′

Table 1
^1H NMR data (500 MHz) in CD_3OD for baculiferins A–H (**2**–**9**) (J in Hz)

	2	3	4	5	6	7	8	9
1	6.86 (d, 1.5)	7.39 (d, 1.5)	7.41 (d, 1.5)	6.86 (d, 1.5)	7.41 (d, 1.5)	6.84 (d, 1.5)	7.43 (d, 1.5)	7.42 (d, 1.5)
1′	6.86 (d, 1.5)	6.86 (d, 1.5)	7.41 (d, 1.5)	6.86 (d, 1.5)	6.88 (d, 1.5)	7.41 (d, 1.5)	7.43 (d, 1.5)	6.89 (d, 1.5)
4	6.83 (d, 8.0)	6.97 (d, 8.0)	7.02 (d, 8.0)	6.84 (d, 8.0)	6.84 (d, 8.0)	6.88 (d, 8.0)	7.03 (d, 8.0)	7.00 (d, 8.3)
4′	6.83 (d, 8.0)	6.87 (d, 8.0)	7.02 (d. 8.0)	6.84 (d. 8.0)	6.98 (d, 8.0)	6.78 (d, 8.0)	7.03 (d, 8.0)	6.89 (d, 8.3)
5	6.72 (dd, 1.5, 8.0)	7.07 (dd, 1.5, 8.0)	7.08 (dd, 1.5, 8.0)	6.71 (dd, 1.5, 8.0)	7.08 (dd, 1.5, 8.0)	6.78 (dd, 1.5, 8.0)	7.09 (dd, 1.5, 8.0)	7.10 (dd, 1.5, 8.3)
5′	6.72 (dd, 1.5, 8.0)	6.76 (dd, 1.5, 8.0)	7.08 (dd, 1.5, 8.0)	6.71 (dd, 1.5, 8.0)	6.78 (dd, 1.5, 8.0)	7.08 (dd, 1.5, 8.0)	7.09 (dd, 1.5, 8.0)	6.78 (dd, 1.5, 8.3)
10	7.58 (s)	7.47 (s)	7.48 (s)	7.57 (s)	7.59 (s)	7.59 (s)	7.58 (s)	7.56 (s)
10′	7.48 (s)	7.47 (s)	7.48 (s)	7.57 (s)	7.49 (s)	7.49 (s)	7.52 (s)	7.56 (s)
13	8.56 (s)	7.85 (s)	7.84 (s)	8.40 (s)	8.54 (s)	8.54 (s)	8.48 (s)	8.36 (s)
13′	8.02 (s)	7.85 (s)	7.84 (s)	8.40 (s)	8.01 (s)	8.01 (s)	7.93 (s)	8.36 (s)
1″	2.99 (t, 6.5)	3.05 (t, 6.5)	3.00 (t, 6.5)	3.00 (t, 7.0)	3.03 (t, 7.0)	3.03 (t, 6.5)	3.04 (t, 6.5)	3.06 (t, 6.5)
2″	2.22 (t, 6.5)	2.20 (t, 6.5)	2.19 (t, 6.5)	2.22 (t, 7.0)	2.20 (t, 7.0)	2.20 (t, 6.5)	2.16 (t, 6.5)	2.20 (t, 6.5)
4″(8″)	6.48 (d, 7.5)	6.50 (d, 8.0)	6.54 (d, 8.0)	6.48 (d, 8.2)	6.53 (d, 8.2)	6.53 (d, 8.2)	6.52 (d, 7.5)	6.51 (d, 7.9)
5″(7″)	6.38 (d, 7.5)	6.35 (d, 8.0)	6.34 (d, 8.0)	6.38 (d, 8.2)	6.37 (d, 8.2)	6.37 (d, 8.2)	6.32 (d, 7.5)	6.33 (d, 7.9)

Table 2
^{13}C NMR data of baculiferins A–O (**2**–**16**) (125 MHz) in CD_3OD

C	2	3	4	5	6	7	8	9	10	11	12	13	14	15	16
1	118.0, d	125.2, d	125.7, d	117.9, d	125.2, d	118.3, d	125.7, d	125.2, d	118.1, d	118.1, d	118.1, d	117.4, d	117.6, d[a]	117.7, d	155.0, s
1′	118.0, d	118.2, d	125.7, d	117.9, d	118.1, d	125.2, d	125.7, d	114.3, d				117.4, d	117.9, d[a]		155.0, s
2	144.8, s	139.8, s	139.6, s	144.8, s	139.8, s	144.6, s	139.5, s	139.8, s	144.8, s	144.8, s	144.8, s	145.0, s	145.0, s	144.7, s	110.3, s
2′	144.8, s	144.5, s	139.6, s	144.8, s	144.6, s	139.8, s	139.5, s	144.6, s				145.0, s	145.0, s		110.3, s
3	145.2, s	148.9, s	149.1, s	145.3, s	149.0, s	145.3, s	149.2, s	148.0, s	145.8, s	143.5, s	145.8, s	145.3, s	145.3, s	145.4, s	122.5, s
3′	145.2, s	145.2, s	149.1, s	145.3, s	145.3, s	149.0, s	149.2, s	145.0, s				145.3, s	145.3, s		122.5, s
4	114.9, d[a]	116.5, d	116.7, s	114.8, d	116.6, d	115.0, d	116.9, d	116.7, d	114.7, d	115.5, d	114.7, d	115.5, d	115.5, d	114.9, d	107.9, s
4′	114.8, d[a]	114.9, d	116.7, s	114.8, d	115.0, d	116.6, d	116.9, d	118.2, d				115.5, d	115.5, d		108.2, s
5	122.7, d	128.6, d	129.0, d	122.7, d	128.6, d	123.3, d	129.1, d	128.6, d	122.6, d	122.5, d	122.6, d	122.1, d	121.6, d	122.2, d	147.9, s
5′	122.7, d	122.7, d	129.0, d	122.7, d	123.3, d	128.6, d	129.1, d	123.3, d				122.1, d	121.6, d		147.9, s
6	124.7, s[a]	124.8, s	129.7, s	124.4, s	124.8, s	124.4, s	124.2, s	124.4, s	123.9, s	123.0, s	123.9, s	124.1, s	124.1, s	123.7, s	105.3, d
6′	124.6, s[a]	124.4, s	129.7, s	124.4, s	124.3, s	124.7, s	124.2, s	123.3, s				124.1, s	124.1, s		104.7, d
7	117.7, s	116.5, s	116.7, s	118.0, s	117.0, s	117.9, s	117.0, s	116.6, s	119.6, s	118.1, s	119.5, s	118.5, s	116.4, s	119.4, s	148.5, s
7′	117.7, s	117.6, s	116.7, s	118.0, s	117.9, s	117.0, s	117.0, s	118.1, s				118.5, s	116.4, s		142.8, s
8	183.4, s	183.6, s[a]	183.7, s	183.7, s	183.4, s	183.6, s	183.7, s	182.0, s	182.0, s	184.5, s	184.4, s	184.4, s	183.8, s	184.6, s	138.5, s
8′	183.9, s	184.0, s[a]	183.7, s	183.7, s	183.9, s	183.1, s	183.2, s	182.0, s	135.0, s	135.0, s	133.9, s	184.4, s	184.3, s	133.9, s	145.0, s
9	130.1, s	131.0, s[a]	130.9, s	130.1, s	130.4, s	130.2, s	130.1, s	130.2, s				130.4, s	129.4, s		117.7, d
9′	130.7, s	130.6, s[a]	130.9, s	130.1, s	130.8, s	130.6, s	130.7, s	130.2, s	122.0, s	124.0, s	122.1, s	130.4, s	130.6, s	122.2, s	111.0, d
10	115.2, d	113.6, d	113.8, d	115.4, d	115.3, d	115.3, d	115.6, d	115.8, d	113.7, d	113.4, d	113.3, d	113.6, d	115.2, d	113.3, d	
10′	114.1, d	113.6, d	113.8, d	115.4, d	114.2, d	114.2, d	114.5, d	115.8, d	124.6, d	116.4, d	115.5, d	113.6, d	114.0, d	116.5, d	
11	150.9, s	147.6, s[a]	147.6, s	151.5, s	150.9, s	150.9, s	151.0, s	151.0, s	147.4, s	147.4, s	147.5, s	147.7, s	151.0, s	147.5, s	
11′	148.0, s	147.5, s[a]	147.6, s	151.5, s	147.9, s	147.9, s	148.1, s	151.0, s	140.0, s	148.0, s	146.7, s	147.7, s	148.7, s	145.4, s	
12	142.6, s	148.8, s[a]	148.8, s	142.6, s	142.6, s	147.9, s	142.7, s	143.0, s	147.4, s	147.4, s	149.6, s	148.9, s	142.7, s	149.6, s	
12′	148.3, s	148.8, s[a]	148.8, s	142.6, s	148.3, s	142.6, s	148.7, s	143.0, s	151.0, s	148.0, s	147.5, s	148.9, s	148.4, s	146.7, s	
13	120.5, d	112.7, d	112.7, d	121.0, d	120.5, d	120.5, d	120.5, d	121.1, d	112.3, d	112.2, d	112.2, d	112.8, d	120.5, d	112.3, d	
13’	113.9, d	112.7, d	112.7, d	121.0, d	113.9, d	113.9, d	113.9, d	121.1, d	117.5, d	114.8, d	116.3, d	112.8, d	114.1, d	115.5, d	
14	122.4, s	123.6, s[a]	123.6, s	122.4, s	122.4, s	122.4, s	122.3, s	122.0, s	123.8, s	123.0, s	123.3, s	123.5, s	122.3, s	123.3, s	
14′	123.0, s	123.5, s[a]	123.6, s	122.4, s	123.3, s	123.3, s	123.2, s	122.0, s	127.9, d	122.5, d	121.6, d	123.5, s	123.0, s	121.6, d	
15	125.2, s	125.1, s[a]	124.5, s[a]	129.6, s	125.2, s	125.2, s	124.9, s	129.0, s	123.9, s	124.0, s	123.6, s	124.8, s	125.0, s	123.7, s	
15′	125.2, s	125.0, s[d]	124.9, s[a]	129.6, s	125.2, s	125.2, s	124.9, s	129.0, s	128.7, s	129.2, s	128.7, s	124.8, s	125.0, s	130.3, s	
16	155.6, s	155.7, s	155.3, s	155.4, s	154.5, s	156.5, s	156.5, s	155.0, s	155.5, s	156.3, s	155.5, s	145.3, s	145.1, s	148.0, s	
16′	154.6, s	154.8, s	155.3, s	155.4, s	154.5, s	156.5, s	156.5, s	155.0, s	171.5, s	174.0, s	171.6, s	145.3, s	145.1, s	172.1, s	
1″	46.5, t	46.8, t	48.5, t	46.6, t	47.0, t	47.0, t	47.0, t	47.0, t	42.9, t	42.5, t	42.8, t	47.1, t	47.1, t	44.5, t	
2″	33.3, t	33.3, t	33.3, t	33.4, t	33.3, t	33.3, t	33.3, t	33.4, t	32.0, t	32.5, t	33.7, t	174.0, s	174, s	174.0, s	
3″	128.3, s	128.5, s	128.6, s	128.3, s	128.5, s	128.5, s	128.4, s	128.6, s	128.7, s	130.1, s	128.7, s				
4″(8″)	129.6, d	129.7, d	129.9, d	129.7, d	129.8, d	129.6, d	129.7, d	129.8, d	127.5, d	118.1, d	129.4, d				
5″(7″)	114.3, d	114.2, d	114.2, d	114.4, d	114.3, d	114.0, d	114.3, d	114.5, d	114.7, d	121.5, d	114.7, d				
6″	155.4, s	155.3, s	155.6, s	155.5, s	155.4, s	155.6, s	155.4, s	155.4, s	155.5, s	151.5, s	155.5, s				

(δ 148.0, s), C-12′ (δ 148.3, s), and C-13′ (δ 113.9, d) of the 11′,12′-dihydroxylated phenyl ring G in purpurone (**1**). C-12 was thus supposed to be substituted by an electron-withdrawing group, possibly an O-sulfate residue. This assumption was supported by the molecular composition of **2** showing a SO_3 group that was absent in purpurone (**1**). Accordingly, the structure of **2** was determined as a 12-O-sulfated purpurone.

Baculiferin B (**3**) had the same molecular formula as **2**, as established by a HRESIMS ion peak at *m*/*z* 776.1076 $[M-H]^-$ (calcd 776.1079) in negative-ion mode, showing that **3** possessed an O-sulfate group, too. The IR, ^1H, and ^{13}C NMR data of **3** (Tables 1 and 2) indicated that it had the same partial structure as purpurone with regard to the rings B, C, D, F, and G. The presence of two individual ABX aromatic spin systems at δ 7.39 (1H, d, J = 1.5 Hz), 6.97 (1H, d, J = 8.0 Hz), and 7.07 (1H, dd, J = 1.5, 8.0 Hz) for ring E, and δ 6.86 (1H, d, J = 1.5 Hz), 6.87 (1H, d, J = 8.0 Hz), 6.76 (1H, dd, J = 1.5, 8.0 Hz) for ring H evidenced the existence of different substitution patterns in these two aromatic rings. HMQC and HMBC analysis led to the assignment of ^1H and ^{13}C NMR data in rings E and F, in which the chemical shifts of C-1 (δ 125.2), C-2 (δ 139.8), and C-3 (δ 148.9) were indicative of an O-sulfate group and a hydroxy function to be substituted at C-2 and C-3 of ring E, respectively, whereas two hydroxy groups were found to be located at C-2′ and C-3′. Thus, the structure of **3** was determined as 2-O-sulfated purpurone.

The NMR spectroscopic data of baculiferins C–F (**4**–**7**) closely resembled those of purpurone (**1**), indicating the presence of the same backbone as purpurone with different substitution patterns.

Baculiferin C (**4**) had a molecular formula of $C_{40}H_{27}NO_{17}S_2$, as determined by HRESIMS and NMR, implying the presence of even two O-sulfate groups. The ^1H NMR spectrum exhibited two duplicated aromatic ABX spin system at δ 7.41 (2H, d, J = 1.5 Hz), 7.08 (2H, dd, J = 1.5, 8.0 Hz), and 7.02 (2H, d, J = 8.0 Hz) for the rings E and H, four aromatic protons represented by two singlets at δ 7.48 (2H, s) and 7.84 (2H, s) for rings D and G, along with the resonances for a *N*-(2-*p*-hydroxyphenyl)ethyl group of ring B, which indicated the presence of a symmetrical structure. The ^{13}C NMR data of C-1/1′ (δ 125.7), C-3/3′ (δ 149.1), and C-2/2′ (δ 139.6) as assigned by HMQC and HMBC investigations were in agreement with O-sulfate groups at C-2 of ring E and C-2′ of ring H, respectively. Therefore, the structure of **4** was determined to be a 2,2′-O-disulfated purpurone.

HRESIMS and NMR data of baculiferin D (**5**) showed that it had the same molecular formula as **4**. ^1H and ^{13}C NMR data (Tables 1 and 2) revealed a symmetrical structure closely related to that of purpurone (**1**), while the NMR data for rings D and G suggested the oxygen functions at C-12 and C-12′ to be sulfated. This was evidenced by the ^{13}C NMR data of C-12 and 12′ (δ 142.6, s) and C-13 and 13′ (δ 121.0, d), which were similar to those of ring D of **2**. The structure of **5** was thus established as 12,12′-O-disulfated purpurone.

Baculiferins E (**6**) and F (**7**) were found to be a 1:1 pair of inseparable isomers. The HRESIMS ion peak at *m*/*z* 856.0668 $[M-H]^-$ (calcd 856.0648) in negative-ion mode corresponded to a molecular formula of $C_{40}H_{27}NO_{17}S_2$, which suggested the presence of two O-sulfate groups. This was confirmed by the negative HRESIMS fragment at *m*/*z* 776.1064 $[M-HSO_3]^-$ (calcd 776.1080). The ^1H and ^{13}C NMR spectra of both compounds (Tables 1 and 2) were almost duplicated, with the exception of a slight differentiation for the conjugated ketone signals at δ 183.1 (s), 183.4 (s), 183.6 (s), and 183.9 (s). The ^1H and ^{13}C NMR data for the rings D and G of **6** and **7** were overlapped and were compatible with those of **2**, hinting at an O-sulfate group to be located at C-12. The chemical shifts assigned to rings E and F by 2D NMR (COSY, HMQC, and HMBC) suggested the oxygen functions at C-2 or C-2′ to be sulfated. Since the remaining NMR data of **6** and **7** were closely similar to those of purpurone (**1**), the structure of **6** was assumed to be 2,12-O-disulfated purpurone, while **7** was 2′,12-O-disulfated purpurone.

The HRESIMS (*m*/*z* 936.0182 $[M-H]^-$, calcd 936.0216) in negative-ion mode and NMR data established the molecular formula of baculiferin G (**8**) as $C_{40}H_{27}NO_{20}S_3$, indicating the presence of even three O-sulfate residues. The ^1H NMR spectrum showed a pair of ABX spin systems at δ 7.43 (2H, d, J = 1.5 Hz), 7.03 (2H, d, J = 8.0 Hz), and 7.09 (2H, dd, J = 1.5, 8.0 Hz), which were assignable to the moieties of aromatic rings E and H. The prominent downfield shifts observed for H-1 (or H-1′), C-1 (or C-1′), and C-3 (or C-3′), together with a pronounced upfield shift of C-2 (or C-2′) (Table 2), permitted the assignment of the O-sulfates to be located at C-2 and C-2′. The third O-sulfate group was deduced to be at C-12 by comparison of the NMR data of ring D with those of **2**. The structure of **8** was thus determined as 2,2′,12-O-trisulfated purpurone.

Baculiferin H (**9**) had the same molecular formula as **8**, as established by HRESIMS data, again possessing three O-sulfate groups. A comparison of the ^1H and ^{13}C NMR data (Tables 1 and 2) revealed its structure to be closely related to that of **6**, but differing in the position of the O-sulfate groups. The overlapped singlets at δ 7.56 (2H, s, H-10, H-10′) and 8.36 (2H, s, H-13, H-13′) indicated a symmetric substructure, and thus an identical substitution pattern in rings D and G. The ^{13}C NMR data of C-11/C-11′ (δ 151.0), C-12/C-12′ (δ 143.0), and C-13/C-13′ (δ 121.1) attributed the sulfate groups to be linked to the oxygen atoms at C-12 and C-12′, whereas C-11 and C-11′ were substituted by free hydroxy groups. The ^1H and ^{13}C NMR spectroscopic data at rings E and H in conjunction with HMQC and HMBC data revealed that an additional O-sulfate group was placed at C-2, while the free hydroxy groups at C-2′ and C-3′ were recognized by their ^{13}C NMR data. Accordingly, the structure of **7** was assigned to the 2,12,12′-O-trisulfate ester of purpurone.

Baculiferin I (**10**) was obtained as a red amorphous powder. The HRESIMS of **10** gave a pseudomolecular ion peak at *m*/*z* 644.0871 $[M-H]^-$ in negative-ion mode, corresponding to the molecular formula of $C_{32}H_{23}NO_{12}S$ (calcd 644.0868), and indicating the presence of 22 units of unsaturation and one O-sulfate group. The UV/VIS bands at 450, 355, 301, 289, and 204 nm showed that the conjugated aromatic system of **10** was blue–shifted as compared to those of **2**–**9**. The ^1H (Table 3) and ^{13}C NMR (Table 2) data of **10** revealed that the structure was closely related to that of ningalin C,[18] except for the chemical shifts of ring G and the aromatic ring linked to the nitrogen. The downfield shifted signals of C-10′ (δ 124.6 d) and C-12′ (δ 151.0, s) along with the upfield shifted resonance of C-11′ (δ 140.0, s) revealed the O-sulfate group to be located at C-11′. In addition, the presence of an aromatic AA′BB′ spin system in **10** instead of the ABX spin system in ningalin C[18] confirmed the presence of an *N*-(2-*p*-hydroxyphenyl)ethyl group. Thus, the structure of **10** was determined to be 11′-O-sulfated 5″-deoxyningalin C.

The molecular formula of baculiferin J (**11**) was the same as that of **10**, as determined through HRESIMS and NMR data. The 1D and 2D NMR spectroscopic data revealed that **11** was closely similar in major parts to the structure of **10**. The only difference was the substituent at C-6″ of ring B, where **11** possessed an O-sulfate group instead of the hydroxy function in **10**. This was evidenced by the ^{13}C NMR resonances of C-4″ and C-8″ and C-6″ in **11** shifted upfield to δ 118.1 (d) and 151.5 (s), whereas the signals of C-5″/C-7″ were shifted downfield to δ 121.5 (d) as compared to those of **10**. In addition, C-11′ of **11** was substituted by a hydroxy function instead of an O-sulfate group as evident from the NMR data. Accordingly, the structure of **11** was assigned as 6″-O-sulfated 5″-dehydroxyningalin C.

The ^1H and ^{13}C NMR data of baculiferin K (**12**) (Tables 1 and 2) indicated that its structure was also closely related to ningalin C.[18] The difference was found in aromatic ring B where an ABX spin system of ningalin C[18] was replaced by an AA′BB′ spin system based on the aromatic signals at δ 6.70 (2H, d, J = 7.9 Hz, H-4″,8″)

Table 3
^{1}H NMR data (500 MHz) for baculiferins I–O (**10**–**16**) (*J* in Hz, CD_3OD)

	10	11	12	13	14	15	16
1	6.85 (br s)	6.84 (br s)	6.85 (br s)	6.65 (br s)	6.71 (br s)	6.67 (d, 1.0)	
1′				6.65 (br s)	6.71 (br s)		
4	6.90 (d, 8.0)	6.96 (d, 8.0)	6.71 (d, 8.0)	6.81 (d, 8.0)	6.81 (d, 7.9)	6.83 (d, 8.0)	
4′				6.81 (d, 8.0)	6.81 (d, 7.9)		
5	6.70 (dd, 8.0, 1.5)	6.92 (dd, 8.0, 1.5)	6.90 (br d, 8.0)	6.55 (br d, 8.0)	6.61 (br d, 7.9)	6.58 (dd, 1.0, 8.0)	
5′				6.55 (br d, 8.0)	6.61 (br d, 7.9)		
6							6.96 (s)
6′							6.89 (s)
9							8.47 (s)
9′							8.00 (s)
10	7.44 (s)	7.46 (s)	7.45 (s)	7.47 (s)	7.59 (s)	7.44 (s)	
10′	7.54 (d, 1.5)	6.88 (br s)	6.90 (br s)	7.47 (s)	7.46 (s)	7.00 (d, 1.0)	
13	7.33 (s)	7.27 (s)	7.25 (s)	7.93 (s)	8.62 (s)	7.31 (s)	
13′	7.08 (d, 8.0)	6.92 (d, 8.0)	6.93 (d, 8.0)	7.93 (s)	8.09 (s)	6.94 (d, 8.0)	
14′	7.18 (dd, 1.5, 8.0)	6.72 (d, 8.0)	6.85 (d, 8.0)			6.92 (dd, 1.5, 8.0)	
1″	3.42 (m) 3.49 (m)	3.60 (t, 7.0)	3.49 (m) 3.37 (t, 7.0)	3.60 (s)	3.52 (s)	3.93 (d, 18.5) 3.94 (d, 18.5)	
2″	2.5 0 (t, 7.0)	2.55 (t, 7.0)	2.50 (t, 7.0)				
4″(8″)	6.71 (d, 7.9)	6.87 (d, 8.5)	6.70 (d, 7.9)				
5″(8″)	6.60 (d, 7.9)	7.15 (d, 8.5)	6.62 (d, 7.9)				
OH-7							9.86 (s)
OH-7′							9.86 (s)
OH-8′							8.58 (s)
NH							14.07 (s)

and 6.62 (2H, d, *J* = 7.9 Hz, H-5″,7″) in **12**, indicating the presence of a *p*-hydroxyphenyl subunit. This assignment was supported by the absence of an oxygen atom in the molecular formula of **12** in comparison to that of ningalin C as determined by HRESIMS. Thus, **12** was a 5″-dehydroxyningalin C.

Baculiferin L (**13**) was obtained as a dark–red amorphous solid. The UV (278, 302, 415 nm), IR (3400, 1627 cm^{-1}), and NMR data indicated that the structure of **13** was closely related to purpurone (**1**). A significant difference was the absence of the *N*-(2-*p*-hydroxyphenyl)ethyl group. In **12** it was replaced by an *N*-2-acetic acid group, which was evident from the singlet of a methylene group at δ 3.60 (2H, s) observed in ^{1}H NMR spectrum and the HMBC correlation between the methylene protons and a carboxylic carbon at δ 174.0 (s, C-2″) and C-16/C-16′ (δ 145.3, s) of the pyrrole nucleus.

Baculiferin M (**14**) had the molecular formula of $C_{34}H_{21}NO_{15}S$ as established by HRESIMS data (*m/z* 716.0706 $[M+H]^+$, calcd 716.0705), indicating the presence of an O-sulfate group. Its ^{1}H and ^{13}C NMR spectroscopic data (Tables 2 and 3) were closely related to those of **13**, except for the substitution at ring D, in which the location of an O-sulfate group at C-12 was recognized by the chemical shifts of C-11 (δ 151.0, s), C-12 (δ 142.7, s), and C-13 (δ 120.5, d).

The NMR spectroscopic data of baculiferin N (**15**) again indicated a structure closely related to ningalin C.[18] A difference was found by the presence of an acetic acid unit, whose α-carbon atom was deduced to be linked to the nitrogen atom of the pyrrole ring, as evident from the presence of the geminal protons at δ 3.93 (1H, d, *J* = 18.5 Hz) and 3.94 (1H, d, *J* = 18.5 Hz) and from their HMBC correlations with a carboxylic carbon at δ 174.0 (s), with C-16 (δ 148.0, s), and with C-16′ (δ 172.1, s).

Baculiferin O (**16**) had the molecular formula $C_{18}H_9NO_{11}S$ as determined from the HRESIMS ion peak at *m/z* 445.9822 $[M-H]^-$ in negative-ion mode and NMR data, and thus contained one O-sulfate group. The ^{1}H NMR spectrum exhibited four aromatic singlets at δ 8.47 (1H, s, H-9), 8.00 (1H, s, H-9′), 6.96 (1H, s, H-6), and 6.89 (1H, s, H-6′), and four D_2O exchangeable protons at δ 14.07 (1H, s, N-H), 9.86 (2H, s, 7, 7′-OH), and 8.58 (1H, s, 8′-OH). The ^{13}C NMR data provided a total of 18 carbon resonances, which partially corresponded to those of ningalin A (**17**), with the exception of the signals of ring D. Thus, the chemical shifts of C-9 (δ 117.7, s) and C-7 (δ 149.5, s) were shifted downfield by ca. 5 ppm, in contrast to that of C-8 (δ 138.5, s), which was shifted upfield by ca. 7 ppm as compared to the corresponding carbons of ring C, indicating C-8 of **16** to be O-sulfated. Thus, **16** was assigned to be as the 8-O-sulfate ester of ningalin A (**17**).

Ningalins including purpurone derivatives are a class of natural alkaloids that are generally recognized to be derived from the amino acid DOPA (3,4-dihydroxyphenylalanine) as a biosynthetic precursor.[19] Retrobiosynthetic analysis suggests that baculiferins A–H (**1**–**9**) are built up from five aromatic amino acid residues. Accordingly, the pyrrole core should be formed by oxidative dimerization of the respective arylpyruvic acid, followed by condensation of the resulting 1,4-diketone with tyramine.[4] The supposed biogenetic pathway via the intermediate 3,4-diarylpyrrole-2,5-dicarboxylic acid is partly evidenced by the structure of the sponge metabolites ningalin A (**17**) and baculiferin O (**16**), which are derived from 3,4-dihydroxyphenylpyruvic acid through ring condensation to form the unsaturated δ-lactone. The asymmetric skeleton of baculiferins I-K (**10**–**12**) is supposed to originate biosynthetically by the condensation of three DOPA residues with tyramine, followed by a similar protocol as in the cases of **1**–**9** (Fig. 2). The *N*-acetic residue in compounds **13**–**15** is assumed to be derived from glycine instead of tyramine in the pyrrole ring formation. The various mono-, bis-, and tris-O-sulfation reactions at the different positions should occur during the later steps of the biosynthesis.

All isolated alkaloids were tested for their activities against the tumor cell lines HCT-8, Bel-7402, BGC-823, A549, and A2780. Compounds **8**, **14**, and **16** showed moderate inhibitory activities (IC_{50} = 19.7, 65.8, and 33.1 μM, respectively), whereas the other substances were only weakly active.

Since derivatives of the structurally closely related to ningalin D possess multidrug resistance reversal activity by inhibition of the human ABC transporter P-glycoprotein,[21] we were interested to find out if these novel compounds exhibit a similar activity. As a model system, we used the facultative human pathogenic fungus *Candida albicans*. The clinical isolate GU5 constitutively overexpresses the two ABC transporters CDR1 and CDR2, which confer multidrug resistance, compared to the genetically related, drug-susceptible isolate GU4 from the same patient.[22] None of the tested compounds did display any antifungal activity against these strains by itself, but all of the substances slightly increased the resistance of the sensitive strain GU4 against brefeldin A, an inhibitor of the

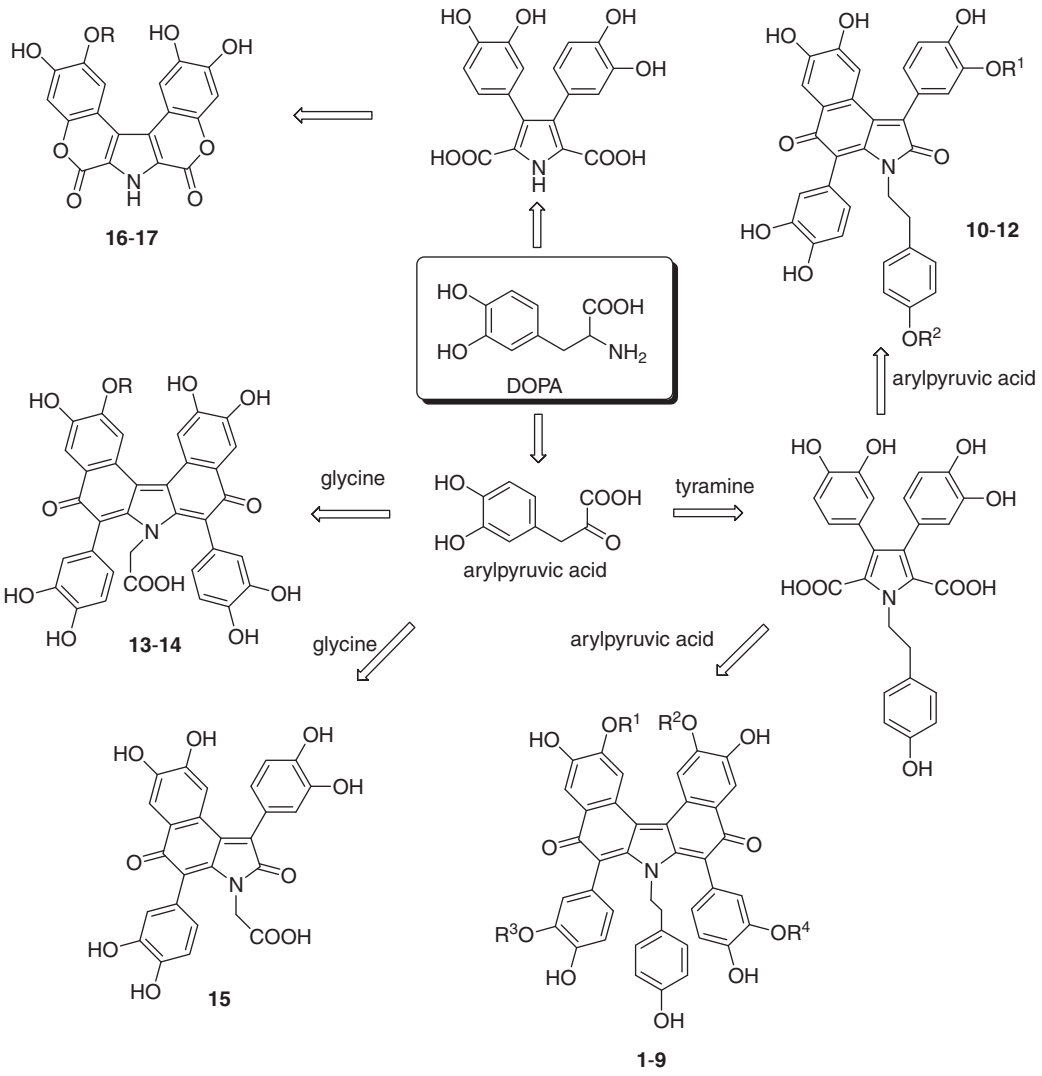

Figure 2. Proposed biosynthetic relationship of baculiferins derived from L-DOPA.

Table 4
MIC (μg/ml) of brefeldin A for the *C. albicans* isolates Gu4 and Gu5 in the presence of a constant concentration of the alkaloids (30 μM) or 1% DMSO (negative control)

	C. albicans strains	
	GU4 (sensitive)	GU5 (resistant)
DMSO	6.3	50
1	12.5	25
2	12.5	50
3	12.5	50
5	12.5	50
6, **7**	12.5	50
14	12.5	50

Table 5
The anti-HIV-1 IIIB activities of baculiferin on MT-4 and MAGI cells

	IC_{50} (μg/mL)	
	MT-4 cells	MAGI cells
1	>25	>25
2	7.6	3.7
3	2.2	1.3
4	8.4	1.2
6–7	4.6	2.7
8	3.2	4.4
9	1.4	1.3
12	5.5	<0.4
13	7.0	4.1
14	5.0	0.2
15	4.4	<0.1

intracellular protein transport. Interestingly, only purpurone (**1**) was able to moderately increase the sensitivity of GU5 to brefeldin A, which is a good substrate for the *Candida* efflux pumps, by a factor of 2 (Table 4). Hence, this alkaloid may inhibit the activity of the *C. albicans* ABC transporters. Nevertheless, none of the novel baculiferins showed a similar activity.

Most remarkably the baculiferins were found to possess potent inhibitory activities against the HIV-1 IIIB virus, which had been encoded in MT4 and MAGI cells (HeLa-CD_4-LTR-β-gal cell line) (Table 5). The anti-HIV-1 IIIB activities were determined by the p24 antigen detection assay. The weak IIIB inhibitory activity of purpurone (**1**) may be explained by its high cytotoxicity against the host cells. Analysis of the structure–activity relationships revealed that the acetic acid group attached to the nitrogen such as in **13**–**15** significantly enhances the inhibitory activity as compared to the effect of the analogues containing *N*-*p*-hydroxyphenylethyl group.

In order to elucidate the mechanism of baculiferins against the HIV-1 virus, their binding activities toward the HIV-1 targets

Table 6
The binding capacity (RU) of baculiferins towards the recombinant proteins of Vif, APOBEC3G, and gp41

Compounds	Concentration (μg/mL)	Vif	APOBEC3G	gp41
1	20	−25.7	−26.3	−23.0
2	20	110.7	170.6	17.1
3	20	152.4	89.7	12.9
4	20	296.4	885.9	115.8
6–7	20	361.9	991.5	108.7
8	20	446.8	571.8	125.1
9	20	259	578.5	76.2
10	20	638.4	/	1351.0
11	20	528.9	765.4	1485.4
12	20	448.4	/	523.3
13	20	1983.2	2170.7	469.0
14	20	1897.0	2463.5	379.7
15	20	596.8	/	952.9
17	20	11.7	/	/

/: Not detected.

including recombinant gp41 (a *trans*-membrane protein of HIV-1), Vif (viral infectivity factor of HIV-1), and human APOBEC3G (an innate intracellular anti-viral factor) using BIAcore were tested. SPR was used to monitor the binding of the molecular interactions. The binding abilities of the alkaloids reacted with target protein are characterized by the respective RU value (response unit, 1 RU = 1 pg/mm^2), that is monitorized as a function of time (sensogram). Generally, the RU value up to the range of 100 is regarded to be meaningful based on the bioassay results obtained from our library with 1000 compounds and medicinal herbs, while the binding capability with up to 500 RU is considered to be significant affinity. Baculiferins containing *N*-acetic acid group, as found in **13**–**14**, had a potent binding affinities toward both Vif (RU >1800) and APOBEC3G (RU >2170) (Table 6). The lactam-type alkaloids **10** and **11** possessed potent affinity toward gp41 (RU >1350). These results suggested that the binding ability of the alkaloids is related to the substitution, whereas the different structural patterns showed selectively binding capability with respective target protein.

These results conducted us to suppose that the mechanism of the anti-HIV-1 IIIB virus activity of the purpurone alkaloids is related to their interaction with the targets Vif, APOBEC3G, and/or gp41. Compounds **13** and **14** have the ability to bind to both targets, viz. Vif and APOBEC3G, whereas the symmetrical structures **1** and **17**, which lack O-sulfate groups, showed no binding capability towards the HIV-1 target proteins. We assume that the O-sulfate containing purpurone-type alkaloids may inhibit the interaction between Vif and APOBEC3G, thus preventing the degradation of APOBEC3G induced by Vif in host cells. In addition, the potent binding activity towards gp41 of **10** and **11** suggested that they may inhibit the virus fusion to host cells.

The DOPA-derived polyaromatic alkaloids have been isolated from widely varying locations and diverse marine organisms such as marine prosobranch mollusks, ascidians, and sponges. Interestingly, the sponge-derived alkaloids mostly possess a tyramine unit[9,10,17,16,20] to replace a dopamine moiety as frequently found from ascidians and other marine organisms, implying a similar biogenetic origin but starting from different precursors in sponges as compared to that in other marine organisms.

Purpurone derived alkaloids containing a glycine moiety have been found in nature for the first time, while DOPA-derived alkaloids with two or three O-sulfate moieties have so far never been reported in the literature.

The bioassay for the cytotoxicity test of the isolated alkaloids towards a series of tumor cell lines revealed that the modification of the phenolic group by a sulfate ester may reduce the cytotoxicity of the parent alkaloids. In addition, the isolated alkaloids showed no inhibitory effect against HIV-1 replication in HEK-293 cells using the VSVG/HIV-luc (293 cells) assay model, a pseudo-type viral system, indicating that the inhibitory pathway of the baculiferins is not specifically targeted to HIV-1 integrase. The potent inhibitory effects against IIIB virus in permissive MT4 and MAGI cells suggested the antagonizing targets of baculiferins not only toward Vif and A3G, but also against other target proteins. Since HIV-1 replication depends on Vif activity only in host cells that express A3G, additional tests in non-permissive cells such as H9 and CEM are required to investigate the affection of interaction between Vif and A3G induced by the alkaloids.

3. Experimental

3.1. General experimental procedures

Optical rotations were recorded on a Perkin–Elmer 341 LC polarimeter. IR spectra were determined on a Thermo Nicolet Nexus 470 FT-IR spectrometer, and UV spectra were recorded on a Shimadzu UV-210A spectrophotometer. ^{1}H and ^{13}C NMR spectra as well as 2D NMR spectra were recorded on a Bruker Avance-500 FT 500 MHz NMR spectrometer using TMS as an internal standard. HRESIMS spectra were recorded on a PE Q-STAR ESITOFMS/MS spectrometer. HF_{254} silica gel for TLC was provided by Sigma Co. Ltd, Sephadex LH-20 (18–110 μm) was obtained from Pharmacia Co., and ODS (50 μm) was purchased from YMC Co.

3.2. Marine sponge

The sponge *I. baculifera* was collected off an inner coral reef (8 m depth) at Hainan Island in the South China Sea, in October 2005. The fresh sample was frozen immediately after collection. The species was identified by Nicole J. de Voogd (National Museum of Natural History). A voucher specimen (HSG-01) is deposited at the State Key Laboratory of Natural and Biomimetic Drugs, Peking University.

3.3. Extraction and isolation

The frozen sponge (600 g, wet wt) was homogenized and extracted with 95% EtOH. The EtOH extract was concentrated in vacuo to yield a residue (9.77 g), which was partitioned between H_2O and EtOAc. The aqueous layer was further extracted with *n*-BuOH. The *n*-BuOH layer was concentrated in vacuo to afford an extract (1.85 g) which was subjected to an ODS column eluting using a gradient of H_2O, MeOH–H_2O (40:60), MeOH–H_2O (70:30), and MeOH to give six fractions (FA–FF). Fraction FC (0.8 g) was chromatographed on an ODS column using a gradient of elution with MeOH–H_2O (3:1) containing 0.1% HOAc to yield a mixture of baculiferins A and B (30 mg), C (**4**, 15.2 mg), D (**5**, 1.8 mg), E and F (**6** and **7**, 144 mg), G (**8**, 13 mg), and H (**9**, 17.4 mg), along with purpurone (**1,** 21.8 mg), baculiferins I (**10**, 9.5 mg), J (**11**, 8.4 mg), K (**12**, 14.4 mg), L (**13**, 30.7 mg), M (**14**, 20.6 mg), N (**15**, 43 mg), O (**16**, 2.0 mg), and ningalin A (**17**, 1.0 mg). The mixture fraction was further resolved by preparative TLC (Silica gel GF_{254} 300–400 mesh, *n*-BuOH–acetic acid–H_2O = 4:4:1) to collect color bands under visible light and to obtain baculiferins A (**2**, 16 mg) and B (**3**, 13.4 mg).

3.3.1. Baculiferin A (2)

Amorphous dark-red solid; UV (MeOH) λ_{max} 262, 276, 327, 508 nm; IR (KBr) ν_{max} 3419, 2925, 1702, 1670, 1561, 1515,1492, 1444, 1294, 1165, 1115, 1023 cm^{-1}; ^{1}H and ^{13}C NMR data (Tables 1 and 2); ESIMS (negative-ion mode) *m/z* 776.2 [M−H]$^-$; HRESIMS (negative-ion mode) *m/z* 776.1072 [M−H]$^-$ (calcd for $C_{40}H_{26}NO_{14}S$, 776.1079).

3.3.2. Baculiferin B (3)

Amorphous dark-red solid; UV (MeOH) λ_{max} 262, 276, 327, 508 nm; IR (KBr) ν_{max} 3420, 2928, 1704, 1675, 1565, 1513, 1446, 1384, 1293, 1117, 1047 cm^{-1}; ^1H and ^{13}C NMR data (Tables 1 and 2); ESIMS (negative-ion mode) *m/z* 776.2 $[M-H]^-$; HRESIMS (negative-ion mode) *m/z* 776.1076 $[M-H]^-$ (calcd for $C_{40}H_{26}NO_{14}S$, 776.1079).

3.3.3. Baculiferin C (4)

Amorphous dark-red solid; UV (MeOH) λ_{max} 262, 276, 327, 508 nm; IR (KBr) ν_{max} 3431, 2925, 1732, 1683, 1628, 1512, 1442, 1297, 1207, 1137, 1049 cm^{-1}; ^1H and ^{13}C NMR data (Tables 1 and 2); HRESIMS (negative-ion mode) *m/z* 856.0640 $[M-H]^-$ (calcd for $C_{40}H_{26}NO_{17}S_2$, 856.0648), *m/z* 776.1074 $[M-HSO_3]^-$ (calcd for $C_{40}H_{26}NO_{14}S$, 776.1080), 681.2987 $[M-SO_3-SO_4]^-$.

3.3.4. Baculiferin D (5)

Amorphous dark-red solid; UV (MeOH) λ_{max} 262, 276, 327, 508 nm; IR (KBr) ν_{max} 3418, 3244, 1731, 1680, 1591, 1559, 1515, 1438, 1408, 1288, 1243, 1167, 1116, 1040 cm^{-1}; ^1H and ^{13}C NMR data (Tables 1 and 2); HRESIMS (negative-ion mode) *m/z* 856.0646 $[M-H]^-$ (calcd for $C_{40}H_{26}NO_{17}S_2$, 856.0648), *m/z* 776.1080 $[M-HSO_3]^-$ (calcd for $C_{40}H_{26}NO_{14}S$, 776.1080).

3.3.5. Baculiferin E (6) and F (7)

Amorphous dark-red solid; UV (MeOH) λ_{max} 262, 276, 327, 508 nm; IR (KBr) ν_{max} 3417, 2927, 1700, 1673, 1563, 1513, 1442, 1401, 1294, 1116, 1043 cm^{-1}; ^1H and ^{13}C NMR data (Tables 1 and 2); ESIMS (negative-ion mode) *m/z* 856.1 $[M-H]^-$, 776.1 $[M-SO_3H]^-$, 696.1 $[M-SO_3H-SO_3]^-$; HRESIMS (negative-ion mode) *m/z* 856.0648 $[M-H]^-$ (calcd for $C_{40}H_{26}NO_{17}S_2$, 856.0647), *m/z* 776.1074 $[M-HSO_3]^-$ (calcd for $C_{40}H_{26}NO_{14}S$, 776.1080).

3.3.6. Baculiferin G (8)

Amorphous dark-red solid; UV (MeOH) λ_{max} 262, 276, 327, 508 nm; IR (KBr) ν_{max} 3432, 2925, 1710, 1628, 1440, 1265, 1025 cm^{-1}; ^1H and ^{13}C NMR data (Tables 1 and 2); ESIMS (negative-ion mode) *m/z* 936.0 $[M-H]^-$; HRESIMS (negative-ion mode) *m/z* 936.0182 $[M-H]^-$ (calcd for $C_{40}H_{26}NO_{20}S_3$, 936.0216), *m/z* 856.0653 $[M-HSO_3]^-$ (calcd for $C_{40}H_{26}NO_{17}S_2$, 856.0648), *m/z* 776.1072 $[M-2(SO_3)-H]^-$ (calcd for $C_{40}H_{26}NO_{14}S$, 776.1080).

3.3.7. Baculiferin H (9)

Amorphous dark-red solid; UV (MeOH) λ_{max} 262, 276, 327, 508 nm; IR (KBr) ν_{max} 3422, 1712, 1673, 1594, 1562, 1514, 1437, 1293, 1117, 1046 cm^{-1}; ^1H and ^{13}C NMR data (Tables 1 and 2); ESIMS (negative-ion mode) *m/z* 936.0 $[M-H]^-$; HRESIMS (negative-ion mode) *m/z* 936.0214 $[M-H]^-$ (calcd for $C_{40}H_{26}NO_{20}S_3$, 936.0216), *m/z* 856.0648 $[M-HSO_3]^-$ (calcd for $C_{40}H_{26}NO_{17}S_2$, 856.0648), *m/z* 776.1076 $[M-2(SO_3)-H]^-$ (calcd for $C_{40}H_{26}NO_{14}S$, 776.1080).

3.3.8. Baculiferin I (10)

Amorphous orange-yellow solid; UV (MeOH) λ_{max} 289 nm; ^1H and ^{13}C NMR data (Tables 2 and 3); ESIMS (negative-ion mode) *m/z* 644.1 $[M-H]^-$; HRESIMS (negative-ion mode) *m/z* 644.0871 $[M-H]^-$ (calcd for $C_{32}H_{22}NO_{12}S$, 644.0868).

3.3.9. Baculiferin J (11)

Amorphous dark-red solid; UV (MeOH) λ_{max} 289 nm; IR (KBr) ν_{max} 3131, 2806, 1730, 1628, 1400, 1349, 1121, 1051, 773 cm^{-1}; ^1H and ^{13}C NMR data (Tables 2 and 3); ESIMS (negative-ion mode) *m/z* 644.1 $[M-H]^-$, 564.1 $[M-HSO_3]^-$; ESIMS *m/z* 668.0 $[M+Na]^+$; HRESIMS $[M+H]^+$ *m/z* 646.1017 $[M+H]^+$ (calcd for $C_{32}H_{24}NO_{12}S$, 646.1014), *m/z* 668.0825 $[M+Na]^+$ (calcd for $C_{32}H_{23}NO_{12}SNa$, 668.0833).

3.3.10. Baculiferin K (12)

Amorphous dark-red solid; UV (MeOH) λ_{max} 226, 475 nm; IR (KBr) ν_{max} 3230, 1710, 1627, 1400, 1348, 1114, 1060, 762 cm^{-1}; ^1H and ^{13}C NMR data (Tables 2 and 3); ESIMS (negative-ion mode) *m/z* 634.1 $[M-H]^-$, 590.1 $[M-COO]^-$; ESIMS *m/z* 658.1 $[M+Na]^+$; HRESIMS *m/z* 636.11277 $[M+H]^+$ (calcd for $C_{34}H_{22}NO_{12}$, 636.1136), 658.0957 $[M+Na]^+$ (calcd for $C_{34}H_{21}NO_{12}Na$, 658.09560).

3.3.11. Baculiferin L (13)

Amorphous dark-red solid; UV (MeOH) λ_{max} 226, 475 nm; IR (KBr) ν_{max} 3430, 2970, 2925, 1710, 1627, 1558, 1449, 1293, 1043 cm^{-1}; ^1H and ^{13}C NMR data (Tables 2 and 3); ESIMS (negative-ion mode) *m/z* 590.1 $[M-CO_2]^-$, *m/z* 634.1 $[M-H]^-$; ESIMS *m/z* 658.1 $[M+Na]^+$; HRESIMS *m/z* 636.1127 $[M+H]^+$ (calcd for $C_{34}H_{22}NO_{12}$, 636.1136), *m/z* 658.0950 $[M+Na]^+$ (calcd 668.0956).

3.3.12. Baculiferin M (14)

Amorphous dark-red solid; UV λ_{max} 278 nm; IR (KBr) ν_{max} 3700–3000, 1628, 1595, 1428, 1383, 1293, 1169, 1025, 878, 798 cm^{-1}; ^1H and ^{13}C NMR data (Tables 2 and 3); ESIMS *m/z* 636.1 $[M-SO_3+H]^+$, *m/z* 716.0 $[M+H]^+$, *m/z* 738.0 $[M+Na]^+$; HRESIMS $[M+H]^+$ *m/z* 716.0706 (calcd for $C_{34}H_{22}NO_{15}S$, 716.0705).

3.3.13. Baculiferin N (15)

Amorphous dark-red solid; UV λ_{max} 278 nm; IR (KBr) ν_{max} 3428–3000, 1695, 1629, 1593, 1513, 1426, 1290, 1169, 1169, 1114, 1053, 877, 796 cm^{-1}; ^1H and ^{13}C NMR data (Tables 2 and 3); ESIMS *m/z* 504.1 $[M+H]^+$; HRESIMS *m/z* 504.0930 $[M+H]^+$ (calcd for $C_{26}H_{16}NO_{10}$, 504.0925).

3.3.14. Baculiferin O (16)

Amorphous light-yellow solid; UV (MeOH) λ_{max} 325, 303, 262 nm; IR (KBr) λ_{max} 3400, 1702, 1617, 1494, 1375, 1256, 1153 cm^{-1}; ^1H and ^{13}C NMR data (Tables 2 and 3); ESIMS (negative-ion mode) *m/z* 446.0 $[M-H]^-$; HRESIMS (negative-ion mode) *m/z* 445.9822 $[M-H]^-$ (calcd for $C_{18}H_8NO_{11}S$, 445.9823).

3.4. Multidrug reversal activity

For the determination of the minimal inhibitory concentration (MIC), serial twofold dilutions of the compounds were performed in DMSO and further diluted with high resolution (HR) medium (14.67 g HR Medium (Oxoid GmbH, Wesel, Germany), 1 g $NaHCO_3$, 0,2 M phosphate buffer pH 7.2) and inoculated with the respective *C. albicans* strain. The MIC was determined according to a previously described method[23] using 40 μM as the highest concentration for the alkaloids in HR medium and a solvent concentration of 1% DMSO. For the determination of the multidrug reversal activity, the MIC of brefeldin A was determined in the same way beginning with a concentration of 50 μM but in the presence or absence of 30 μM of the respective compounds. All data gained in two independent experiments with duplicates achieved identical results.

3.5. Test for anti-HIV-1 IIIB activities using MT-4 cells

The 5×10^6 MT-4 cells were harvested by centrifugation, and then were infected with 1 mL 10000 $TCID_{50}$ HIV-1 IIIB in RPMI 1640 medium. After incubation at 37 °C for 2 h, the cell suspensions were centrifuged at 1500 rpm. The supernatant was discarded and washed with RPMI 1640 medium once, then centrifuged and re-suspended with 10 mL RPMI 1640 medium. 5×10^4 HIV-infected or mock-infected MT-4 cell suspensions were added in 100 μL volumes to the wells of a flat-bottom 96-well culture plate. Varying dilutions of the test compounds in RPMI 1640 medium were added in 100 μL volumes to the wells. The highest

concentration of the test compounds was 250 μg/mL, then diluted fivefold serially. Five dilutions and four duplicates were applied for each dilution. The wells only with virus-infected cells and without compounds were used as a viral control and the wells only with mock-infected cells, without virus or compounds, were used as a cell control. The cell cultures were then incubated at 37 °C in 5% CO_2 humidified atmosphere for 5 d. On the third day, half of the supernatant in each well was refreshed with the correspondingly diluted compounds or RPMI 1640 medium. Growth and morphology were analyzed every day. On the third or fourth day, syncytium formation was observed in the virus-control wells and no morphological change in the cell-control wells. On the fifth day, the supernatant was harvested and detected for p24 antigen, representing the propagation of the HIV viruses. The p24 concentrations were compared between the test compounds and the virus control, and the inhibitive rate was calculated with the formula listed:

$$\text{Inhibitive rate } (\%) = ([\text{p24}]_{\text{control}} - [\text{p24}]_{\text{testing cpd}})/[\text{p24}]_{\text{control}}$$

$$[\text{p24}] = \text{concentration of p24 in pg/mL}$$

The anti-HIV-1 IIIB activities of the test compounds were determined by a p24 antigen detection assay. After plotting the inhibitive rate values of the test compound (*Y* axis) against their corresponding concentrations (*X* axis), the 50% inhibitive concentration (IC_{50}) was calculated by using a linear regression analysis. Four duplicates were conducted for each sample.

3.6. Test for anti-HIV-1 IIIB activities using MAGI cells

The MAGI test, also called single life cycle, reflects only one round of infection. The viral life cycle was synchronized. The test compound was added at different hours post the virus inoculation to observe which stage of the viral life cycle could be inhibited by the compound. The cells used were derived from the HeLa cell line, which expresses high levels of CD4 and contains a single integrated copy of a β-galactosidase gene under the control of HIV-1 LTR. This cell line, called HeLa-CD_4-LTR-β-gal, can be used to determine quantitatively the titer of HIV strains. The inhibitive rate of the test compound was calculated and the stage upon which the test compound acted was determined.

The HeLa-CD_4-LTR-β-gal indicator cells were plated in 96-well plates at 6000 cells per well. The highest concentration of the test compounds was 200 μg/mL, then diluted by fourfold serially. Five dilutions and four duplicates were applied for each dilution. The wells containing only virus-infected cells and no compounds were used as the viral control and the wells equipped only with mock-infected cells and without virus or compounds were used as the cell control. The supernatant in the test wells and the viral-control wells was discarded and infected with 100 μL 2000 $TCID_{50}$ HIV-1 IIIB. Then 100 μL of the diluted solutions of the test compounds as described above were added to the wells, making the final concentration of the test compounds decreased by half. The cell cultures were incubated at 37 °C in 5% CO_2 humidified atmosphere for 40–48 h, then fixed and stained. The blue cells were counted under an inverted microscope. Four duplicates were conducted for each sample.

3.7. Target test using BIAcore

The recombinant gp41, Vif, or APOBEC3G was immobilized on the sensor Chip CM5 surface in each flow cell separately. When the test compound was injected at a constant flow, the interaction and detection occurred on the chip surface. Thus, the BIAcore instrument could detect the binding capacity of the test compound with the recombinant gp41, Vif, or APOBEC3G.

Acknowledgments

This project was supported by grants from the National Hi-Tech Development Project (863 project) (No. 2006DFA31100, 2007AA09Z448, 2008AA09Z405), NSFC (No. 30930109), National Key Innovation Project (2009ZX09501-014, DYXM-115-02-2-09), and by the Deutsche Forschungsgemeinschaft (SFB 630, projects A2, B2, and Z1/QM). We thank S. Sologub (SFB 630, project Z1) for the performance of the mdr-reversal activity tests and Dr. Nicole J. de Voogd (National Museum of Natural History, The Netherlands) for the sponge taxonomy.

A. Supplementary data

Supplementary data associated with this article can be found, in the online version, at doi:10.1016/j.bmc.2010.06.052.

References and notes

1. John, W. B.; Brent, R. C.; Murray, H. G. M.; Peter, T. N.; Michele, R. P. *Nat. Prod. Rep.* **2005**, *22*, 15.
2. Reddy, S. M.; Srinivasulu, M.; Satyanarayana, N.; Kondapi, A. K.; Venkateswarlu, Y. *Tetrahedron* **2005**, *61*, 9242.
3. Fan, H.; Peng, J.; Hamann, M. T.; Hu, J. *Chem. Rev.* **2008**, *108*, 264.
4. Bailly, C. *Curr. Med. Chem.* **2004**, *4*, 363.
5. Andersen, R. J.; Faulkner, D. J.; He, C.; Van Duyne, G. D.; Clardy, J. *J. Am. Chem. Soc.* **1985**, *107*, 5492.
6. Cantrell, C. L.; Groweiss, A.; Gustafson, K. R.; Boyd, M. R. *Nat. Prod. Lett.* **1999**, *14*, 39.
7. Carroll, A. R.; Bowden, B. F.; Coll, J. C. *Aust. J. Chem.* **1993**, *46*, 489.
8. Lindquist, N.; Fenical, W.; Van Duyne, G. D.; Clardy, J. *J. Org. Chem.* **1988**, *53*, 4570.
9. Kock, M.; Reif, B.; Fenical, W.; Griesinger, C. *Tetrahedron Lett.* **1996**, *37*, 363.
10. Urban, S.; Butler, M. S.; Capon, R. J. *Aust. J. Chem.* **1994**, *47*, 1919.
11. Urban, S.; Hobbs, L.; Hooper, J. N. A.; Capon, R. J. *Aust. J. Chem.* **1995**, *48*, 1491.
12. Urban, S.; Capon, R. J. *Aust. J. Chem.* **1996**, *49*, 711.
13. Reddy, M. V. R.; Faulkner, D. J.; Venkateswarlu, Y.; Rao, M. R. *Tetrahedron* **1997**, *53*, 3457.
14. Davis, R. A.; Carroll, A. R.; Pierens, G. K.; Quinn, R. J. *J. Nat. Prod.* **1999**, *62*, 419.
15. Yoshida, W. Y.; Lee, K. K.; Carroll, A. R.; Scheuer, P. J. *Helv. Chim. Acta* **1992**, *75*, 1721.
16. Palermo, J. A.; Brasco, M. F. R.; Seldes, A. M. *Tetrahedron* **1996**, *52*, 2727.
17. Isabelle, C.; Bernard, B.; Philippe, A. *J. Nat. Prod.* **2000**, *63*, 981.
18. Chen, G. W.; Francis, T.; Thureen, D. R.; Offen, P. H.; Pierce, N. J.; Westley, J. W.; Johnson, R. K. *J. Org. Chem.* **1993**, *58*, 2544.
19. Kang, H.; Fenical, W. *J. Org. Chem.* **1997**, *62*, 3254.
20. Reddy, M. V. R.; Rao, M. R.; Rhodes, D.; Hansen, M. S. T.; Kathleen, R.; Bushman, F. D.; Venkateswarlu, Y.; Faulkner, D. J. *J. Med. Chem.* **1999**, *42*, 1901.
21. Hamasaki, A.; Zimpleman, J. M.; Hwang, I.; Boger, D. L. *J. Am. Chem. Soc.* **2005**, *127*, 10767.
22. Franz, R.; Ruhnke, M.; Morschhäuser, J. *Mycoses* **1999**, *42*, 453.
23. Ruhnke, M.; Eigler, A.; Tennagen, I.; Geiseler, B.; Engelmann, E.; Trautmann, M. *J. Clin. Microbiol.* **1994**, *32*, 2092.